Journal of Plant Physiology 212 (2017) 94–104

Contents lists available at ScienceDirect

Journal of Plant Physiology

journal homepage: www.elsevier.com/locate/jplph

Research paper

Spatio-temporal dynamics in global rice gene expression (*Oryza sativa* L.) in response to high ammonium stress

Li Sun[a], Dongwei Di[a], Guangjie Li[a], Herbert J. Kronzucker[b,c], Weiming Shi[a,*]

[a] State Key Laboratory of Soil and Sustainable Agriculture, Institute of Soil Science, Chinese Academy of Sciences, Nanjing 210008, China
[b] Department of Biological Sciences, University of Toronto, 1265 Military Trail, Toronto, ON, M1C 1A4, Canada
[c] School of BioSciences, The University of Melbourne, Parkville, VIC 3010, Australia

ARTICLE INFO

Article history:
Received 7 January 2017
Received in revised form 20 February 2017
Accepted 21 February 2017
Available online 22 February 2017

Keywords:
Ammonium (NH_4^+) toxicity
Rice (*Oryza sativa* L.)
RNA-Seq (Quantification) profiling
Spatial-temporal specificity

ABSTRACT

Ammonium (NH_4^+) is the predominant nitrogen (N) source in many natural and agricultural ecosystems, including flooded rice fields. While rice is known as an NH_4^+-tolerant species, it nevertheless suffers NH_4^+ toxicity at elevated soil concentrations. NH_4^+ excess rapidly leads to the disturbance of various physiological processes that ultimately inhibit shoot and root growth. However, the global transcriptomic response to NH_4^+ stress in rice has not been examined. In this study, we mapped the spatio-temporal specificity of gene expression profiles in rice under excess NH_4^+ and the changes in gene expression in root and shoot at various time points by RNA-Seq (Quantification) using Illumina HiSeqTM 2000. By comparative analysis, 307 and 675 genes were found to be up-regulated after 4 h and 12 h of NH_4^+ exposure in the root, respectively. In the shoot, 167 genes were up-regulated at 4 h, compared with 320 at 12 h. According to KEGG analysis, up-regulated DEGs mainly participate in phenylpropanoid (such as flavonoid) and amino acid (such as proline, cysteine, and methionine) metabolism, which is believed to improve NH_4^+ stress tolerance through adjustment of energy metabolism in the shoot, while defense and signaling pathways, guiding whole-plant acclimation, play the leading role in the root. We furthermore critically assessed the roles of key phytohormones, and found abscisic acid (ABA) and ethylene (ET) to be the major regulatory molecules responding to excess NH_4^+ and activating the MAPK (mitogen-activated protein kinase) signal-transduction pathway. Moreover, we found up-regulated hormone-associated genes are involved in regulating flavonoid biosynthesis and are regulated by tissue flavonoid accumulation.

© 2017 Elsevier GmbH. All rights reserved.

1. Introduction

In plants, nitrate (NO_3^-) and ammonium (NH_4^+) are the two major inorganic nitrogen (N) forms that are directly absorbed by the root system. Even though NH_4^+ is frequently more readily absorbed by roots and its assimilation requires less energy than that of NO_3^- (Kronzucker et al., 2000), only a few species perform well when NH_4^+ is the sole N source, while most of them suffer NH_4^+ toxicity when exposed to excess NH_4^+ as the sole N source (Britto and Kronzucker, 2002). NH_4^+ toxicity is typically visible in stunted root systems and in chlorosis of leaves, accompanied by dramatically reduced tissue accumulation of mineral cations and increased root NH_4^+ fluxes (Britto et al., 2001; Britto and Kronzucker, 2002; Li et al., 2014).

Knowledge of NH_4^+ toxicity has greatly expanded in recent years, in particular in terms of signaling transmission and molecular and physiological targets in Arabidopsis (*Arabidopsis thaliana*) (Li et al., 2014; Bittsánszky et al., 2015). Many NH_4^+ toxicity- associated genes have been identified, such as *HSN1/VTC1*, *GAS1/ARG1*, *XBAT32*, *ETO1*, *DPMS*1, *AMOS1/EGY1*, *AMOS2*, *CAP1*, *SLAH3*, and *Gln1.2*, all of which were associated with sensitivity to NH_4^+, while *TRH1*, *AMT1.3*, *AUX1*, and *ETR1* were shown as critical to resistance to NH_4^+ (Bai et al., 2014; Li et al., 2014; Zheng et al., 2015; Guan et al., 2016). Some analyses of NH_4^+ toxicity at the whole genome-wide level have also been made. For instance, Yang et al. (2015a) revealed a coordinated regulation of carbohydrate and amino acid metabolism under high NH_4^+ for short periods (up to several hours) of exposure in rice shoots and roots. Furthermore, Yang et al. (2015b) showed that NH_4^+-induced nutritional and metabolic imbalances can be partially overcome by elevated root auxin levels in Arabidopsis under high NH_4^+. Wang et al. (2016) carried out transcriptomic and physiological analyses of common duckweed in response to NH_4^+ toxicity to elucidate the participation of

* Corresponding author.
E-mail address: wmshi@issas.ac.cn (W. Shi).

http://dx.doi.org/10.1016/j.jplph.2017.02.006
0176-1617/© 2017 Elsevier GmbH. All rights reserved.

oxidative damage, lignin biosynthesis, phenylpropanoid metabolism, and programmed cell death (PCD). However, the majority of NH_4^+ toxicity research has focused on one gene or one signaling pathway at a time and typically only examined the root or shoot in isolation. Much less attention has been paid to whole-plant analysis, signaling transduction from root to shoot, and feedback signaling from shoot to root. Another infrequently examined aspect is the time course of toxicity development. Due to such restrictions, critical adjustments in signaling and metabolism in the context of whole-plant acclimation and adaptation to NH_4^+ stress may have remained invisible. It is well known that stress-priming can enable plant cells to sense very low levels of a stimulus and allow for initiation of resistance systems when challenged initially, thereafter enabling long-term adaptations to chronic or recurring stress (Conrath, 2011; Conrath et al., 2015). Mapping out the early stress response is, therefore, also critical. Thus, with the goal of characterizing regulatory networks, a spatio-temporal analysis of the key changes incurred as a result of NH_4^+ exposure is needed.

Rice is an NH_4^+-tolerant model crop known to grow well in soil environments characterized by high NH_4^+ and has indeed been often been described as an NH_4^+ specialist (Kronzucker et al., 1999; Kronzucker et al., 2000). Nevertheless, even rice has been shown to suffer toxicity at elevated levels of NH_4^+, albeit at a much higher threshold than other cereals such as wheat or barley (Szczerba et al., 2008; Balkos et al., 2010; Britto et al., 2014). Rice also offers well-established genetic resources for the application of systems biology (Chandran and Jung, 2014). Some genes related to excess NH_4^+ were previously identified in rice: Xie et al. (2015) identified *OsSE5* (*HO1*), which is involved in the heme-heme oxygenase 1(heme-HO1) antioxidant system and may improve tolerance to excess NH_4^+ by optimizing antioxidant defense. Moreover, *OsPTR6* could increase rice growth by increasing NH_4^+ transporter expression and GS activity under high NH_4^+ supply (Fan et al., 2014). In addition, *OsAMT1.1* transgenic rice has shown superior growth and higher yield under elevated NH_4^+ conditions (Ranathunge et al., 2014). Recently, Ma et al. (2016) showed GABA (γ-aminobutyric acid) can alleviate NH_4^+ toxicity by limiting NH_4^+ accumulation in rice. However, NH_4^+ toxicity in rice remains poorly characterized overall, and examinations both at the whole-plant and subcellular level are clearly required (Bittsánszky et al., 2015). On the other hand, mechanisms of NH_4^+ toxicity in rice seem to differ from other plants such as Arabidopsis, which is a strongly NH_4^+-sensitive species, or species such as the common duckweed, whose fronds and roots are directly exposed to NH_4^+ in their natural environment (Wang et al., 2016). Thus, identifying the molecular and physiological mechanisms in the rice response to excess NH_4^+ are important prerequisites to helping crop biotechnologists identify traits for improving rice germplasms that perform well at high NH_4^+.

Because of the importance of rice as a global commodity, as the dominant calorie source directly consumed by humans, and the potential threat to its production deriving from elevated soil NH_4^+ content in heavily fertilized soils, a better understanding of rice tolerance to excess NH_4^+ is clearly needed. To this end, we undertook a comprehensive analysis of global changes in the rice genome during the stages of NH_4^+ toxicity development using RNA-Seq (Quantification). We produced RNA-Seq data from shoots and roots sampled from two-week-old seedlings that were initially grown for 4 h and 12 h and supplied with 7.5 mM $(NH_4)_2SO_4$, which allowed us to examine the response to the onset of excess NH_4^+ that may be invisible to analyses conducted at only one time point. Gene Ontology (GO) enrichment and Kyoto Encyclopedia of Genes and Genomes (KEGG) pathway enrichment were used to identify the important biological processes and crucial signaling pathways operating in rice shoot and root tissues.

2. Materials and methods

2.1. Plant growth conditions and stress treatments

Seeds of *Oryza sativa* ssp. japonica were surface-sterilized with 1% sodium hypochlorite for 10 min, washed extensively with distilled water, and then germinated in distilled water at 28 °C for 2 days. Germinated seeds were transferred into a growth chamber (16/8 h (28/25 °C) day/night, a light intensity of 400 μmol m^{-2} s^{-1}, and a constant relative humidity of 70%) in 4.0-l vessels containing aerated modified Johnson's solution (2 mM $MgSO_4$; 1 mM $CaCl_2$; 0.5 mM KCl; 0.3 mM NaH_2PO_4; 0.1 mM Fe-EDTA; 20 μM H_3BO_3; 9 μM $MnCl_2$; 1.5 μM $CuSO_4$; 1.5 μM $ZnSO_4$; 0.5 μM Na_2MoO_4, pH 5.5), either under N-sufficient [1 mM $(NH_4)_2SO_4$] or N-excess [2.5 mM, 5 mM, 7.5 mM, 10 mM and 20 mM $(NH_4)_2SO_4$)] conditions for an additional 14 days. Then seedling length was measured, and fresh biomass of shoot and root was determined. Solutions were exchanged every 12 h to ensure that plants remained at a nutritional steady state in the hydroponic system. For the high-NH_4^+ (HN) treatment, seedlings were first grown on N-sufficient solution for 14 days. Then, seedlings were transferred to an N-starvation solution (no N) for another 3 days to deplete N in vivo and ensure the maximization of NH_4^+ absorption by seedlings. After that, seedlings were grown on 7.5 mM $(NH_4)_2SO_4$ (HN) solutions. Samples (three biological replicates) of shoots and roots were taken separately at 0, 4, and 12 h after the imposition of HN treatments, frozen immediately, and stored at −80 °C until RNA-Seq (Quantification) analysis.

2.2. Tissue ammonium (NH_4^+) content determination

Seedlings were harvested and desorbed for 5 min in 10 mM $CaSO_4$ to remove extracellular NH_4^+. Roots and shoots were separated and weighed, then transferred to 10-ml polypropylene tubes and frozen in liquid N_2 for storage at −80 °C. Approximately 1 g of root or shoot tissue was homogenized under liquid N_2 using a mortar and pestle, followed by the addition of 6 ml of formic acid (10 mM) for the purpose of extracting NH_4^+. 1 ml homogenate was centrifuged at 12,000 rpm at 4 °C for 10 min. The supernatant was then transferred to 2-ml polypropylene tubes with 0.45-μm nylon filters (Costar, Corning Inc., USA) and centrifuged at 12,000 rpm at 4 °C for 5 min. The resulting supernatant was analyzed by a modified o-phthalaldehyde (OPA) method (Balkos et al., 2010) to determine total tissue NH_4^+ content: 100 ml of OPA reagent was prepared by combining 200 mM potassium phosphate buffer (composed of equimolar amounts of KH_2PO_4 and K_2HPO_4) and 3.75 mM OPA. Then, the solution pH was adjusted to 7 with 1 M NaOH. 2 mM 2-mercaptoethanol was added into the solution one day before use. For sample testing, 200 μl aliquots of tissue extract were combined with 2 ml of OPA reagent. The color was allowed to develop in the dark for 15 min at room temperature, and sample absorbance was measured at 410 nm.

2.3. RNA extraction, library preparation, and RNA sequencing ‘

Total RNA was isolated with TRIzol reagent (Invitrogen, USA) according to protocol of the manufacturer. Then, mRNA was purified from total RNA using the Oligotex mRNA Midi Kit (Qiagen, Germany). After that, the total RNA samples were treated with DNase I to degrade any possible DNA contamination. Then, mRNA was enriched using oligo (dT) magnetic beads. Mixed with the fragmentation buffer, mRNA was fragmented into short fragments. Then, the first strands of cDNA were synthesized using random hexamer-primer. Buffer, dNTPs, RNase H, and DNA polymerase I were added to synthesize the second strand. Double-strand cDNA was purified with magnetic beads. End reparation and 3′-end

single nucleotide A (adenine) addition were then performed. Finally, sequencing adaptors were ligated to the fragments. The fragments were enriched by PCR amplification. During the QC (quality control) step, Agilent 2100 Bioanalyzer and ABI Step One Plus Real-Time PCR System were used to qualify and quantify the sample library. Then, the library products were sequenced via Illumina HiSeqTM 2000.

2.4. Mapping of RNA-Seq reads

Primary sequencing data, produced by Illumina HiSeqTM 2000 and called "raw reads", were subjected to quality control (QC) to determine if a re-sequencing step was needed. After QC, raw reads were filtered into clean reads, which would be aligned to the reference sequences. After filtering, the remaining reads, called "clean reads", were stored in FASTQ format (Cock et al., 2010). We used Bowtie2 (Langmead et al., 2009) to map clean reads to reference genes and used BWA (Li and Durbin., 2009) to reference the full genome. Only uniquely mapped reads were used in the analysis. The gene expression (FPKM) levels were estimated using the following formula:

$$FPKM = \frac{10^6 C}{NL/10^3}$$

Given is the expression of gene A; C is the number of fragments uniquely aligned to gene A; N is the total number of fragments uniquely aligned to all genes; L is the number of bases in gene A. The calculated gene expression can be directly used for comparing gene expression patterns among samples.

2.5. Screening differentially expressed genes (DEGs) using NOISeq

NOISeq method can screen differentially expressed genes (DEGs) between two groups. First, NOISeq uses a sample's gene expression in each group to calculate log2 (fold change) M and the absolute different value D of all pair conditions to build a noise distribution model:

$$M^i = \log_2\left(\frac{x_1^i}{x_1^i}\right) \text{ and } D^i = |x_1^i - x_2^i|$$

Second, for gene A, NOISeq computes its average expression "Control_avg" in the control group and the average expression "Treat_avg" in the treatment group. Then, the fold change (M_A = log2((Control_avg)/(Treat_avg))) and absolute different value D (D_A = |Congrol_avg- Treat_avg|) are obtained. If M_A and D_A diverge from the noise distribution model markedly, gene A will be defined as a DEG. There is a probability value to assess how M_A and D_A both diverge from the noise distribution model:

$$P_A = P(M_A \geq \{M\} \&\& D_A \geq \{D\})$$

Finally, we screened differentially expressed genes according to the following default criteria: Fold change ≥2 and diverge probability ≥0.8.

2.6. Gene ontology (GO) function annotation

Gene Ontology (GO) classifications for a set of genes were performed by the Web Gene Ontology Annotation Plot (WEGO). All genes in the rice genome were used as background for significance testing. We first mapped all DEGs to GO terms in the database (http://www.geneontology.org/), calculating gene numbers for every term. Then we used a hyper geometric test to find significantly enriched GO terms in the input list of DEGs based on 'GO:Term Finder' (http://www.yeastgenome.org/help/analyze/go-term-finder), which is described as follows:

$$P = 1 - \sum_{i=0}^{m-1} \frac{\binom{M}{i}\binom{N-M}{n-i}}{\binom{N}{n}}$$

N is the number of all genes with GO annotation; n is the number of DEGs in N; M is the number of all genes annotated to certain GO terms; m is the number of DEGs in M. The calculated *p*-value goes through Bonferroni correction (Abdi, 2007), taking corrected *p*-value ≤0.05 as a threshold. GO terms fulfilling this condition are defined as significantly enriched GO terms in DEGs. This analysis is able to recognize the main biological functions that DEGs exercise. Blast2GO was further used to assign biological functions, cellular components, and cellular processes to transcripts.

2.7. Kyoto encyclopedia of genes and genomes (KEGG) pathway enrichment analysis

Mapped sequences were annotated against the Kyoto Encyclopedia of Genes and Genomes (KEGG) database (http://www.genome.jp/kegg/) to obtain enzyme commission (EC) numbers. To obtain KEGG Pathway-Maps, the EC numbers were then mapped to the KEGG biochemical pathways. GO terms for genes from the rice (version 6.1) reference genome were downloaded. Pathway-based analysis helps to further understand the biological functions encoded by the various genes identified. KEGG (the major public pathway-related database) was used to perform pathway enrichment analysis of DEGs. The formula used for calculations was the same as that used for GO analysis:

$$P = 1 - \sum_{i=0}^{m-1} \frac{\binom{M}{i}\binom{N-M}{n-i}}{\binom{N}{n}}$$

Here, N is the number of all genes with KEGG annotation; n is the number of DEGs in N; M is the number of all genes annotated to specific pathways; m is the number of DEGs in M.

2.8. Quantitative real-Time PCR

Total RNA was extracted from shoots and roots harvested at the specified time points with TRIzol reagent (Invitrogen, USA) and treated with RNase-free DNaseI (Promega). Total RNA (2 μg) was used for reverse transcription with M-MLV Reverse Transcriptase (Promega), and the cDNA samples were diluted two-fold. For qRT-PCR, triplicate quantitative assays were performed on each cDNA dilution with SYBR Premix Ex Taq (TaKaRa) and a CFX Manager sequence detection system according to the following protocol: denaturation at 95 °C with 30 s for initiation, denaturation at 95 °C for 10 s, 40 cycles of amplification, annealing and extension at 55 °C/60 °C for 30 s. Specificity of the amplification was checked using a melting curve performed from 65 to 95 °C, as well as sequencing of the amplification. Three independent replicates were performed per experiment, and the means and corresponding standard errors were calculated. Ubiquitin protein (UBI1) was used as a normalization control. Primer sequences were as listed in Supplementary Table S2.

2.9. Statistical analysis

All statistical analyses were conducted using SPSS version 13.0, and one-way ANOVA was performed with a homogeneity of variance test, followed by an LSD test to check for quantitative differences between treatments. $P < 0.05$ was set as the significance cut-off.

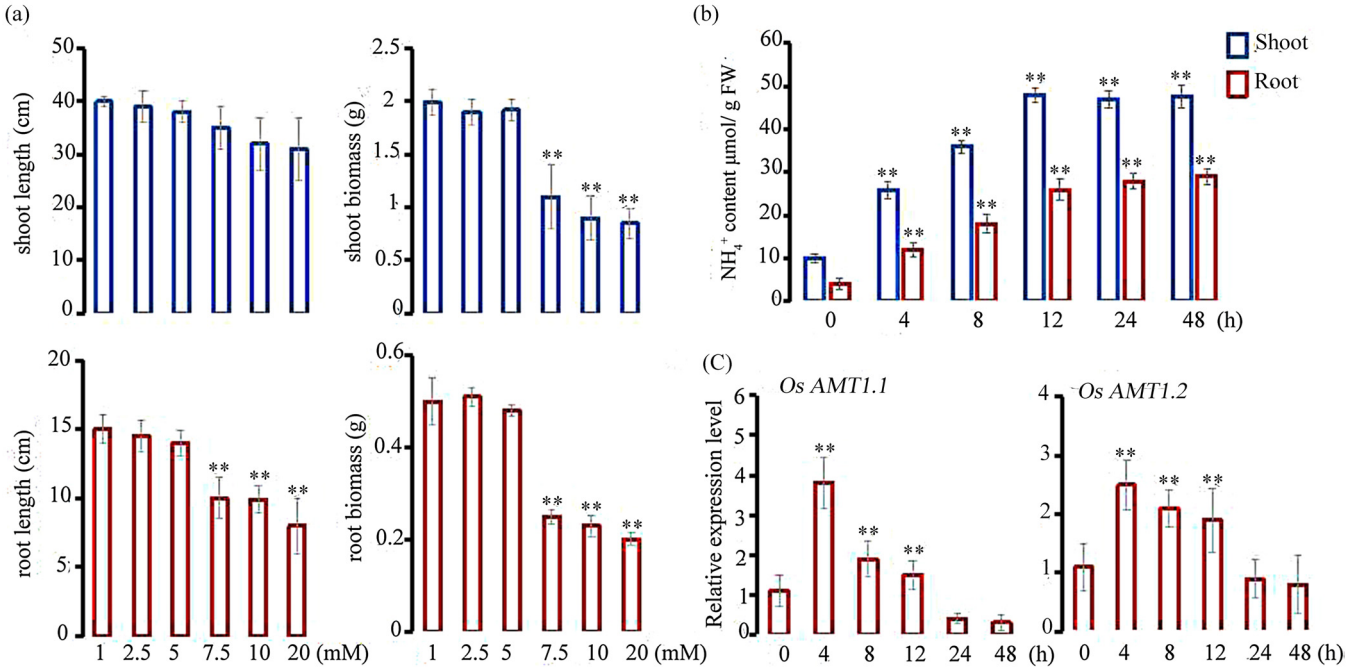

Fig. 1. Rice phenotypic responses to different NH_4^+ concentrations. (a) The length and biomass of shoot and root under different NH_4^+ conditions (HN). (b) NH_4^+ concentrations of root and shoot under NH_4^+ stress [7.5 mM $(NH_4)_2SO_4$]. (c) The expression levels of NH_4^+ transporter genes OsAMT1.1 and OsAMT1.2 in the root at 7.5 mM $(NH_4)_2SO_4$. Bars indicate standard errors of the mean of 30 plants. Mean values are shown for a sample size of three replicates.

3. Results

3.1. Phenotypic response of rice to excess NH_4^+

In order to determine the highest NH_4^+ concentration rice could tolerate in our experimental conditions, we chose 1, 2.5, 5, 7.5, 10, and 20 mM $(NH_4)_2SO_4$, and monitored the changes in shoot and root lengths and fresh biomass in 14-day-old plants. The results showed that root growth was retarded at 7.5 mM $(NH_4)_2SO_4$. Shoot length did not show any significant difference, but biomass in both shoot and root were decreased by 50% at 7.5 mM $(NH_4)_2SO_4$ (Fig. 1a). Thus, 7.5 mM $(NH_4)_2SO_4$ was chosen as HN.

We measured changes in internal NH_4^+ concentration in shoots and roots prior to and following treatments at various different time points, up to 48 h. Simultaneously, we analyzed the *OsAMT1* gene family by qRT-PCR, which is known to code for high-affinity NH_4^+ transporters (Sonoda et al., 2003). NH_4^+ concentrations in roots and shoots began to increase between 4 h to 12 h in the root, after which the NH_4^+ concentration did not show further differences (Fig. 1b). Meanwhile, transcripts of *OsAMT1.1*and *OsAMT1.2* in the root showed clear induction and reached the highest levels at 4 h, with *OsAMT1.2* maintaining high levels up to 12 h (Fig. 1c). Therefore, we chose 0, 4, and 12 h for RNA-Seq analysis.

3.2. Identification of DEGs in response to NH_4^+ excess

We sequenced 18 samples using RNA-Seq technology, and the average number of raw sequencing reads and clean reads are shown in Supplementary Table S1. The unique mapping ratio with reference gene and the average genome mapping ratio were more than 80% (Supplementary Table S1). To judge the significance of the gene expression differences and to define DEGs, two filtering criteria were used in our data analysis: a two-fold or greater change in transcript level between any two time points and a P-value <0.05. Four profiles (4S:4-h-Shoot/12S:12-h-Shoot and 4R:4-h-Root/12R:12-h-Root) were utilized to depict the transcripts of all DEGs in three replicates at 4 h and 12 h in both shoots and roots.

307 and 675 genes were up-regulated and 216 and 684 genes were down-regulated, based on the analysis of 4S and 12S, respectively (Fig. 2a). In roots, 167 and 31 genes were up-regulated and down-regulated, respectively, for 4R compared with 320 and 96 genes for 12R (Fig. 2a). To identify both unique and common genes showing differential expression patterns at the time points in both shoot and root, numbers were calculated and presented using a Venn diagram (Fig. 2b). The results show that 367 and 153 DEGs were commonly induced on shoot and root, respectively. 5 DEGs were regulated in both shoot and root, demonstrating a progressive biological process. Moreover, 133 and 932 DEGs were unique to the shoot, compared to 25 and 200 that were uniquely induced in the root at 4 h and 12 h, respectively (Fig. 2b). In addition, GO enrichment analysis focusing on the categories of biological processes was used to classify the biological functions of DEGs under HN. As shown in Supplementary Fig. S1, the DEGs were classified into three main categories including biological process, cellular component, and molecular function (corrected P-value <0.05). Cell, cell parts, and organelle under cellular component were the three most well represented subcategories.

3.3. Roots and shoots exhibit distinct spatio-specific codes in response to excess NH_4^+

We first used KEGG enrichment analysis to classify the cardinal biological processes and crucial regulatory genes in the root under the HN condition. As shown in Fig. 3a, the foremost processes that were engaged fell into the categories of plant-pathogen interaction and hormone signaling pathways. The plant-pathogen interaction category vis-a-vis the hypersensitive response (HR), especially programmed cell death (PCD) and cell wall enforcement, was up-regulated, followed by hormone signaling transduction, especially that involving the MAPK signaling pathway and defense-related genes (Fig. 3a and Supplementary File S1). Concomitantly, transcripts involved in amino acid metabolism were up-regulated, mainly those which take part in lipid metabolism, including a small subset of genes involved in fatty acid elongation and

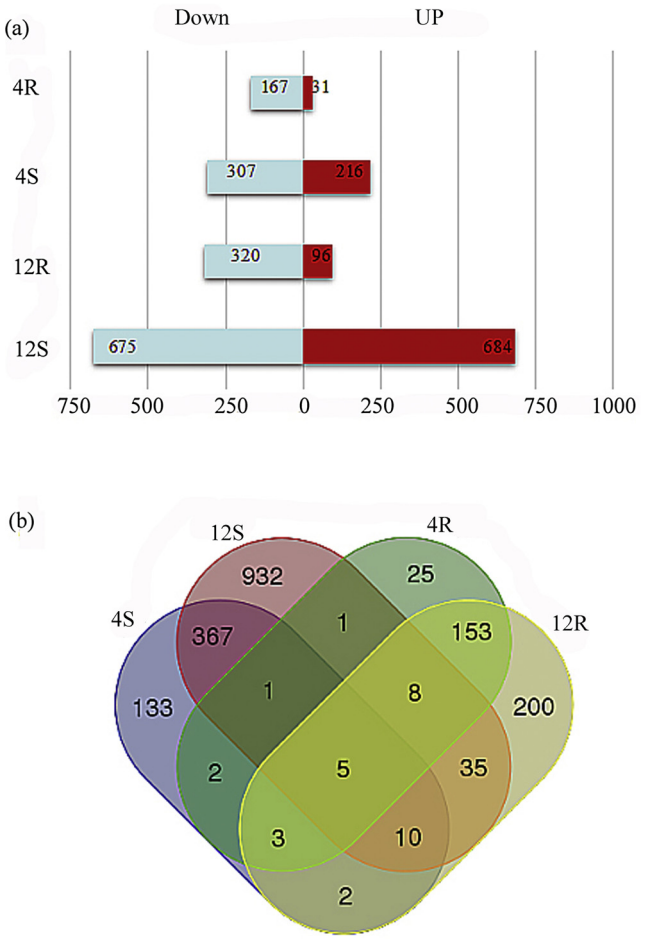

Fig. 2. Numbers and Venn diagram display of DEGs in rice shoot and root under HN treatments. **(a)** DEG number in shoot and root at 4 h and 12 h. (R value <0.05 and genes with the regulation ratio log ≥ 2 or ≤−2 were selected). Blue: down-regulated. Red: up-regulated. **(b)** Venn diagram showing the overlapping number of DEGs in shoot and root at different time points. (Blue:4S, Pink:12S, Green:4R, Yellow:12R). 4S:4-h-Shoot; 4R:4-h-Root; 12S:12-h-Shoot; 12R:4-h-Root.(For interpretation of the references to colour in this figure legend, the reader is referred to the web version of this article.)

desaturation in the plastid (Fig. 3a and Supplementary File S1). In addition, transcripts that map to glutathione, ascorbate, and aldehyde metabolism were up-regulated as well, accompanied by oxidative stress marker genes (Fig. 3a and Supplementary File S1). Energy metabolism pathways, such as oxidative phosphorylation and fructose and mannose metabolism, were up-regulated notably. In addition, we found the transcripts of ABA and ET biosynthesis to be up-regulated in the root under HN (Fig. 3a and Supplementary File S1).

In comparison with the root, the shoot must receive signals on soil stresses from the root indirectly. As shown in Fig. 3b, genes related to chemical defense metabolism were the most significantly enhanced. Moreover, as in the root, genes related to phenylpropanoid biosynthesis were crucial within the secondary metabolism category (Fig. 3b and Supplementary File S2). We found eight genes were constitutively up-regulated under HN. All these genes belong to peroxidases involved in flavonoid oxidation, cinnamyl alcohol dehydrogenase involved in lignin biosynthesis, beta-glucosidase involved in a variety of processes such as the release of phytohormones from inactive glycosides, and the cytochrome P450 gene CYP98A/C3′H known to play an essential role in the regulation of phenylpropanoid metabolism. Moreover, transcripts related to key photosynthesis genes were increased (Supplementary File S2). In accordance with the latter, genes in starch and sucrose metabolism and fructose and mannose metabolism were up-regulated as well (Supplementary File S2). We also found increased expression levels of genes involved in the ascorbate-glutathione antioxidant system and lipid metabolism, similar to what was revealed in the root. Interestingly, we found transcripts involved in GABA biosynthesis to be up-regulated 2.8-fold in the shoot under HN. Among hormone pathways, only ABA biosynthesis genes were seen to be up-regulated in the shoot under HN (Supplementary File S2).

3.4. Temporal-specific codes in the shoot and root under excess NH_4^+

With prolonged stress, root and shoot revealed temporal-specific codes. The top 20 KEGG pathways with the highest representation of DEGs at the two time points in root and shoot are shown in Fig. 4. In the root, the two most up-regulated DEGs belonged to the plant-pathogen interaction pathway and to the defense-associated hormone [gibberellin (GA), abscisic acid (ABA), ethylene (ET), jasmonic acid (JA), and salicylic acid (SA)] signaling category at 4 h of exposure, which was followed by increasing carbohydrate and acid metabolism (Fig. 4 and Supplementary File S1). With increasing time of HN treatment, plant-pathogen defense signaling and ET, GA, and SA hormone signaling transcripts increased a further 2-fold by 12 h, while ABA and JA did not change significantly. We also found antioxidant components, such as glutathione metabolism and ascorbate and aldarate metabolism, to be up-regulated more than 2-fold by 12 h, accompanied by increased energy metabolism signaling related to galactose metabolism. In addition, transcripts relating to secondary metabolite biosynthesis, such as pyruvate, phenylalanine metabolism, and flavonoid biosynthesis, increased significantly (Fig. 4 and Supplementary File S1).

Maximum transcript numbers relating to the biosynthesis of phenylpropanoids, such as lignin and flavonoids, were seen with increasing time of NH_4^+ stress at shoot (Fig. 4 and Supplementary File S2). Energy metabolism, most evidently starch and sucrose metabolism, increased at 4 h under HN, and was especially visible in amino sugar and nucleotide sugar metabolism. Other than this, energy metabolism, such as photosynthesis and glycolysis/gluconeogenesis metabolism, was up-regulated by 12 h. Consistent with this, growth regulation genes were up-regulated distinctly, while circadian rhythm gene expression was maximized at 4 h (Fig. 4 and Supplementary File S2). Simultaneously, transcripts of ascorbate and lignin biosynthesis increased up to 7-fold. Additionally, glutathione metabolism increased (Fig. 4 and Supplementary File S2). We also found genes involved in carotenoid biosynthesis enhanced distinctly at 4 h compared to 12 h, as shown in Fig. 4 and Supplementary File S2. Even though hormone signaling was not changed significantly, some transcription factors (TFs) were up-regulated (Supplementary File S2).

3.5. TFs (transcription Factors) in hormone regulation upon exposure to excess NH_4^+

TFs are of special interest since they are capable of coordinating the expression of several or many downstream targets genes and, hence, entire metabolic and developmental pathways. As shown in Supplementary File S3, 32 TFs and 43 TFs were induced in the root at 4 h and 12 h, respectively, and 17 TFs and 32 TFs in the shoot at these time points. TFs also revealed spatio-temporal specificity under HN. As shown in Supplementary File S3, three genes were only induced at 4 h in the root, while 14 genes were expressed at 12 h. Likewise, five genes were only induced at 4 h in the shoot, while 22 genes were expressed at 12 h. More importantly, most of the up-regulated TFs showed marked (>4-fold) changes in

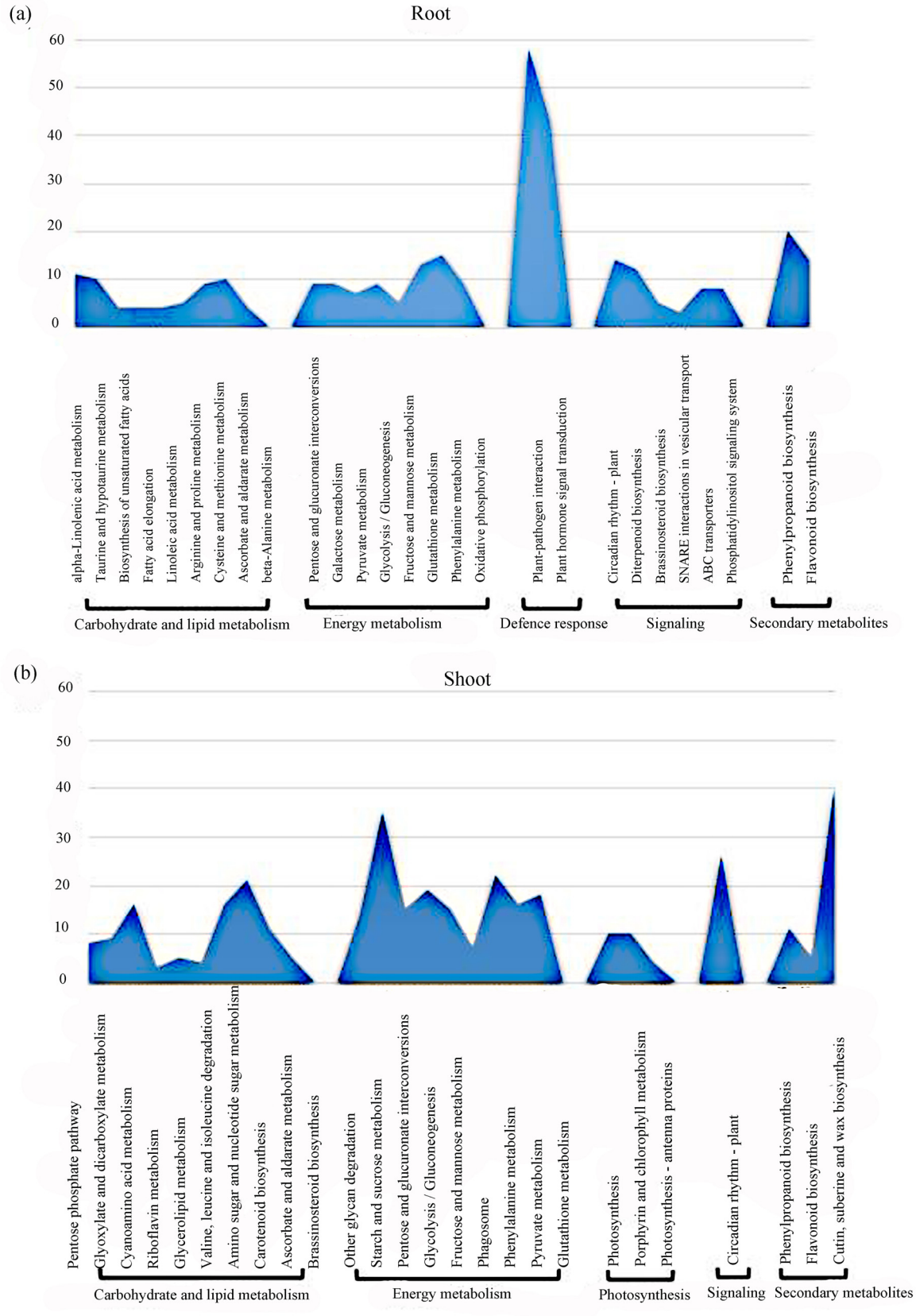

Fig. 3. Spatial specificity in root and shoot under HN treatments. **(a)** The major defense and metabolism pathways in the root under HN. **(b)** The crucial metabolism pathways in the shoot under HN condition. R value <0.05 and genes with the regulation ratio log ≥ 2 or ≤ −2 were selected.

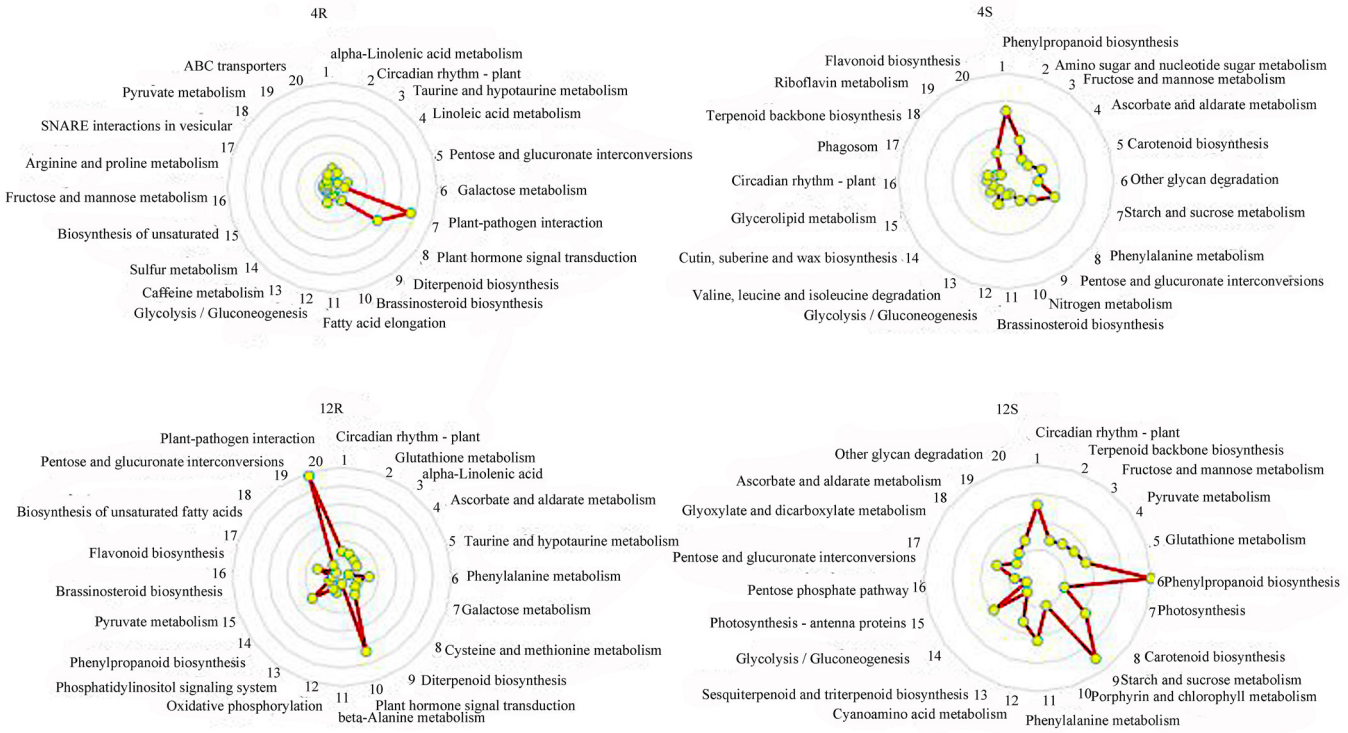

Fig. 4. Temporal specificity in root and shoot under HN treatments. The top 20 metabolism pathways were selected; R value <0.05 and genes with the regulation ratio log ≥ 2 or ≤-2 were selected. 4S:4-h-Shoot; 4R:4-h-Root; 12S:12-h-Shoot; 12R:4-h-Root.

transcript abundance in response to HN condition. Some interesting example are depicted in Table 1. The TFs uncovered mainly belong to the C2C2(Zn)CO-like zinc finger family and the AP2/EREBP and MYB families. Two of the G2-like (MYB-like) GARP, involved in phosphorous metabolism, abaxial cell identity, and photosynthetic development, were induced under HN. Five MYB genes showed marked changes in transcript abundance under HN. AP2/EREBP proteins,known to play important roles in plant growth and development throughout the plant life cycle especially in response to environmental stresses, were induced under HN (3-fold higher transcript level under HN). In addition, as shown in Table 1, many of the TFs are involved in MAPK-based signal transduction. Moreover, 30 TFs related to protein degradation and modification via the ubiquitin proteasome pathway were induced. To confirm the gene expression profiling data obtained from RNA-seq, qRT-PCR analysis of the selected TFs was performed as shown in Supplementary Fig. S2. The differential expression observed with RNA-seq was generally confirmed with qRT-PCR data.

3.6. Expression changes of homologous NH_4^+-related genes of rice in response to excess NH_4^+

Many NH_4^+-toxicity-related genes in Arabidopsis have been identified, most of which are involved in root growth regulation under excess NH_4^+. To identify the expression changes of their homologues in rice, we first identified the homologues genes in rice using the Basic Local Alignment Search Tool (BLAST) from the National Center for Biotechnology Information (NCBI) as shown in Table 2. We found not all homologous were induced under HN conditions. Two of the Os *VTC1* genes were up-regulated, while only LOC_Os01g62840 was enhanced from 4 h to 12 h, as was the case with Os *AMOS1*. The expression levels of two Os *SLAH3* genes were increased at 4 h and 12 h. However, Os *CAP1* was only induced at 4 h and decreased at 12 h, while Os *AMT1.3* and one of Os *Gln1.2* were only expressed at 12 h. Os *AUX1* has five homologous genes in the rice genome. Under HN, LOC_Os03g14080 was induced at 4 h and 12 h in the shoot, while LOC_Os05g37470 was only expressed at 12 h. Nevertheless, the expression levels of LOC_Os10g05690 and LOC_Os11g06820 increased at 4 h and 12 h with small changes. Unfortunately we did not find obvious change in LOC_Os01g63770 under HN. To confirm the gene expression profiling data obtained by RNA-seq, qRT-PCR analysis was carried out as shown in Supplementary Fig. S3. The differential expression observed with RNA-seq was generally confirmed with qRT-PCR data.

4. Discussion

The present study unravels the participation of the key signaling networks at the genome-wide level in rice in response to NH_4^+ stress, which is hoped to promote general understanding of the regulation of NH_4^+ tolerance at the level of the whole plant. In total, 1469 DEGs were up-regulated, while 1027 were down-regulated, under HN (Fig. 2b). GO and KEGG enrichment analysis revealed that the up-regulated genes mainly fell into cellular function and metabolic process categories, and gene transcription indicated that some important physiological or "housekeeping" functions increased significantly (Supplementary File S1 and S2).

4.1. Spatio-temporal specificity of gene expression in rice under NH_4^+ toxicity

The root system is first in line when plants are challenged with stresses from the soil environment and, thus, must respond rapidly to such stress signals to enable acclimation and tolerance. Among the earliest defense responses in the root is the strengthening of pre-existing physical and chemical barriers. Recent studies have shown densely packed uniseriate sclerenchyma cells close to the root apex strengthen their barriers to reduce the excessive NH_4^+

Table 1
Distribution and function of TFs under HN conditions. R value <0.05 and genes with the regulation ratio log ≥ 2 were selected.

Gene ID	Annotation information	log2Ratio under HN	
4R			
LOC_Os09g26780/Os09g0439200	JAZ8/OsTIFY10c(jasmonate ZIM domain-containing protein 8)/**C2C2(Zn)CO-like zinc finger family**/acts as a repressor of JA signaling in rice	3	–
LOC_Os03g27280/Os03g0390200	SnRK2/SAPK1(osmotic stress/abscisic acid-activated protein kinase 1)/**serine/threonine-protein kinase/**MAPK signaling pathway	2.6	–
12R			
LOC_Os07g03590/Os07g0126401	PR1(pathogenesis-related protein 1)/**pathogenesis-related protein PRB1-3-like**/MAPK signaling pathway	3	–
LOC_Os06g13320/Os06g0241100	BRI1(protein brassinosteroid insensitive 1)/**G-type lectin S-receptor-like serine/threonine-protein kinase SD2-5**/Signal transduction	6.8	–
LOC_Os09g37330/Os09g0545300	SAUR36 (SAUR family protein)/auxin-responsive protein SAUR36/SMALL AUXIN UP RNA 36/Signal transduction	5	–
LOC_Os03g64260/Os03g0860100	1 **ERF1(ethylene-responsive transcription factor 1)/**AP2 domain containing protein**/MAPK signaling pathway**	8.2	–
LOC_Os05g33940/Os05g0410200	GID1(gibberellin receptor GID1)/**Cell death associated protein**/Signal transduction	3	–
4S			
LOC_Os03g58350/Os03g0797800	IAA14(Indoleacetic acid-induced protein 14)/**Auxin-responsive protein IAA14**/auxin-activated signal transduction	–	13.2
LOC_Os03g08330/Os03g0181100	JAZ10 (jasmonateZIM domain-containing protein 10)/**Protein TIFY 11b**/jasmonic acid mediated signaling pathway	–	6
LOC_Os02g27220/Os02g0471500	OsPP2C14(protein phosphatase 2C 14)/**serine/threonine phosphatase activity**/MAPK signaling pathway	–	4.2
LOC_Os02g10860/Os02g0203000	ABF(ABA responsive element binding factor)/gibberellic acid mediated signaling pathway/positive regulation of circadian rhythm	–	5.2
12S			
LOC_Os05g43690/Os05g0512600	CRE1/AHK2/3/4(histidine kinase 2/3/4-cytokinin receptor)/**hydrolase activity,polysaccharide binding**/Signal transduction	–	10.6
LOC_Os05g29030/Os05g0358500	OsPP2C48(protein phosphatase 2C 48)/**serine/threonine phosphatase activity**/MAPK signaling pathway	–	5.6
LOC_Os12g05660/Os12g0152800	TGA(transcription factor TGA)/**protein tyrosine/serine/threonine phosphatase activity**/Signal transduction	–	5
LOC_Os02g05630/Os02g0149800	OsPP2C10 protein phosphatase 2C 10)/**serine/threonine phosphatase activity**/PPM-type phosphatase/MAPK signaling pathway	–	4
LOC_Os01g13740/Os01g0239000	ARR-B/OsGLK2(Probable transcription factor GLK2, Golden2-like protein 2)/**MYB-typ**e/Signal transduction	–	5
LOC_Os06g24070/Os06g0348800	ARR-B/OsGLK1(Probable transcription factor GLK1, Golden2-like protein 1)/**MYB-type**/Signal transduction	–	4.4
LOC_Os02g53200/Os02g0771700	CRE1/AHK2/3/4(histidine kinase 2/3/4-cytokinin receptor)/**hydrolase activity,polysaccharide binding**/Putative beta-1,3-glucanase/Signal transduction	–	7.8

Table 2
The expression levels of homologous genes in rice under HN treatments.

Gene name	Gene ID	Arabidopsis homologous gene	4S	4R	12S	12R
OsVTC1	LOC_Os03g16150/Os03g0268400	*VTC1*(Glucose-1-phosphate adenylyltransferase)	2.6	−0.12	2.23	0.04
	LOC_Os08g13930/Os08g0237200		0.6	0.45	1.72	0.29
	LOC_Os01g62840/Os01g0847200		5.8	0.64	7.31	0.61
OsARG1	LOC_Os01g32870/Os01g0512100	*ARG1* (Chaperone DnaJ-domain protein)	0.34	0.02	0.46	−0.04
	LOC_Os02g50760/Os02g0741100		1.2	0.02	0.78	−0.45
OsAMOS1	LOC_Os03g57840/Os03g0792400	*AMOS1* (Ethylene dependent gravitropism deficient and yellow green1/Peptidase M50 protein)	2.4	0.8	7.6	−2.61
OsAUX1	LOC_Os01g63770/Os01g0856500	*AUX1* (Auxin influx carrier protein 1)	0.86	0.11	0.44	0.12
	LOC_Os03g14080/Os03g0244600		9.46	−1.02	9.47	−1.07
	LOC_Os05g37470/Os05g0447200		−0.54	−0.99	2.63	−1.48
	LOC_Os10g05690/Os10g0147400		7.14	0.002	6.72	−1.18
	LOC_Os11g06820/Os11g0169200		3.78	−0.12	4.6	0.02
OsXBAT32	LOC_Os02g54860/Os02g0791200	*XBAT32* (Ring-type E3 ligase)	0.44	0.02	0.01	0.2
OsETO1	LOC_Os03g18360/Os03g0294700	*ETO1* [Ethylene overproducer 1/tetratricopeptide repeat (TPR)-containing protein]	1.16	0.22	0.71	−0.03
OsDPMS1	LOC_Os03g60939/Os03g0824400	*DPMS*1 (dolicholphosphate mannose synthase 1/Nucleotide-diphospho-sugar transferases protein)	0.008	−0.41	0.27	0.02
OsCAP1	LOC_Os03g55210/Os03g0759600	*CAP1*{[Ca(2+)] cyt-associated protein kinase}	2.83	−0.99	1.4	0.51
OsGln1.2	LOC_Os02g50240/Os02g0735200	*Gln1.2* (Cytosolic glutamine synthetase 1.2)	0.74	−0.26	2.96	0.48
	LOC_Os03g12290/Os03g0223400		0.07	−1.15	1.5	−0.54
OsAMT1.3	LOC_Os04g43070/Os04g0509600	*AMT1.3* (Ammonium transporter 1.3)	1.19	0.29	5.6	1.2
OsETR1	LOC_Os03g49500/Os03g0701700	*ETR1* (Ethylene response 1)	0.28	0.23	0.45	0.44
OsSLAH3	Os05g0219900	*SLAH3* (Slow anion channels/SLAC1-homolog protein 3/S-type anion channel)	8.32	1.12	3.68	0.86
	LOC_Os01g12680/Os01g0226600		2.65	0.54	6.48	−3.7
OsTRH1	LOC_Os07g48130/Os07g0679000	*TRH1* (Potassium transporter protein)	1.15	0.48	−0.4	0.09

transport into the rice root (Ranathunge et al., 2016). Moreover, the ascorbate- glutathione cycle, one of the important processes for free radical detoxification under biotic or abiotic stress, is frequently engaged early (Domínguez-Valdivia et al., 2008; Wang et al., 2016). In our study, many genes involved in these defense responses were indeed up-regulated significantly (Fig. 3 and Supplementary File S1). These underscore that physical and chemical barriers might play an important role for rice in the staging of the early response to NH_4^+ toxicity, as appears to be the case with other stresses. With increasing stress exposure time, many stress-related signaling pathways were activated, in particular those involving phytohormones. It is known that ABA and ET signaling pathways are involved in Arabidopsis under NH_4^+ toxicity in the root, but this had not been examined in rice, as a model system of NH_4^+-tolerant plants. We found *ABA2*, centrally involved in ABA biosynthesis, and *ACS* and *ACO*, involved in ET biosynthesis, were up-regulated under HN (Supplementary File S3). This suggests ABA and ET are crucial signaling molecules in rice, as they are in NH_4^+-sensitive Arabidopsis (Li et al., 2014). Correspondingly, we found the key ABA- and ET-response elements, *ABFs* and *ERFs*, were up-regulated as well (Supplementary File S3). Thus, the phytohormones ABA and ET may be the major regulatory signaling molecules in the root under HN. Furthermore, these signaling pathways belong to the MAPK-signaling transduction pathway. MAPK signaling pathways are present in both the cytoplasm and the nucleus and are involved in a variety of crucial processes such as osmoregulation, cell growth, and differentiation (Mishra et al., 2006). Therefore, we conclude that the MAPK transduction pathway, regulated by ABA and ET, plays a central role in the early stress response of rice to NH_4^+ stress in the root. The root not only reinforces its physical and chemical responses to retard damage incurred from NH_4^+ stress below-ground, but also activates ABA and ET signaling to the shoot, possibly through the MAPK transduction pathway, and, in such a way, orchestrates defense signals sensitization and transmission.

An array of signals is typically generated when roots are exposed to an environmental stress. Some, but not all, are then conveyed to the shoot via the transpiration stream. Here, we found many transcripts relating to MAPK signal transduction in the shoot under HN (Supplementary File S3). This reveals that the transduction of NH_4^+ toxicity signaling from root to shoot might occur through the MAPK signaling pathway. Meanwhile, most transcripts involved in phenylpropanoid biosynthesis were up-regulated after 4 h and 12 h of NH_4^+ exposure in the shoot under HN (Supplementary File S2). In higher plants, phenylpropanoid metabolism is the gateway for the production of a great variety of secondary metabolites, such as flavonoids, isoflavonoids, lignin, anthocyanin, phytoalexins, and phenolic esters, all of which are critical players in development, structural protection, defense responses, and tolerance to abiotic stimuli (Naoumkina et al., 2010). Induction of flavonoid synthesis in response to environmental stimuli can alter auxin transport to allow for adjustments in plant growth and development to stress (Buer et al., 2007; Peer and Murphy, 2007). Nguyen et al. (2013) also found ABA to modulate the biosynthesis of flavonoids and alter the direction of polar auxin transport with the consequence of suppressing lateral root growth in plants suffering from drought stress. We also found the expression level of *ABA2* transcripts, critical to ABA biosynthesis, up-regulated in the shoot under HN (Supplementary File S3). Thus, we speculate that feedback signaling from shoot to root in the early stages of NH_4^+ exposure was via the MAPK transduction pathway, regulated by ABA. The shoot only perceives NH_4^+ stress signals from the root indirectly, as it is not typically directly exposed. Thus, intracellular physiological defense responses, such as the biosynthesis of secondary metabolites, assume a primary role in this process. These metabolites can regulate the polar transport of auxin and then regulate root growth in response to the imposed stress. Therefore, in the early NH_4^+ stress defense process, the root acts as a command center to activate and deliver stress-related defense signals, while the shoot engages in response and feedback.

4.2. Metabolism adjustments play an important role in NH_4^+ resistance

Environmental stress in plants also alters or disrupts metabolic homeostasis. In stressed conditions, plant metabolism must be modified to produce compounds necessary to cope with and adapt to the stress (Shulaev et al., 2008). Hence, plants have to devote significant resources to stress defense (Heil and Baldwin, 2002). In agreement with this expectation, many transcripts in carbohydrate metabolism pathways were up-regulated in both the root and shoot under HN (Supplementary File S1 and S2). However, rice, as an NH_4^+-tolerant crop, must have especially well-responding energy metabolism with regard to this stress. Indeed, components of energy metabolism in response to HN increased considerably. Together with the amplification of the light reactions of photosynthesis, transcripts involved in the generation of ATP and NAD(P)H, which might be necessary to facilitate enhanced NH_4^+ resistance, were up-regulated (Supplementary File S1 and S2). It is well known that adjustment of ATP formation and its utilization for synthesis of compatible solutes, and enhanced energy metabolism in general, are strategies plants use to cope with salt stress (Zhang et al., 2013; Zhao et al., 2013). In addition, elevated levels of amino acids and organic acids in plant cells have been correlated with enhanced stress tolerance through the scavenging of free radicals and protecting enzymes (Flowers and Colmer, 2015). Proline accumulation is a well-known measure to improve osmoprotection in particular and is seen under a variety of stresses (Saxena et al., 2013). Congruously, transcripts in proline metabolism were increased under HN (Supplementary File S1 and S2). In addition, proline is also involved in maintaining the NADP+/NADPH ratios required for normal metabolism (Hare et al., 1998). However, in Arabidopsis, proline accumulation has also been shown to have negative impacts, leading to cell toxicity under high temperature conditions (Lv et al., 2011). In rice, proline may serve as a positive factor in adapting to HN stress in the early stages of NH_4^+ toxicity.

4.3. Role of phytohormones in NH_4^+ tolerance

Phytohormones are molecules produced in very low concentrations but work as chemical messengers to communicate cellular activities and coordinate various signal transduction pathways during abiotic stress, integrating external as well as internal stimuli (Peleg and Blumwald, 2011; Vob et al., 2014). It has been reported that auxin, ET, and ABA are involved in NH_4^+-responsive pathways in Arabidopsis (Li et al., 2014). Endogenous ABA levels increase rapidly, activate specific signaling pathways, and modify gene expression to enable plants to survive under adverse environmental conditions (Cutler et al., 2010). However, it has not been hitherto examined whether ABA regulation is involved in response to NH_4^+ toxicity in rice. In our study, the ABA biosynthesis genes *ABA1*, *ABA2*, and *ABI1* were up-regulated in the rice root and shoot under HN (Supplementary File S3). Meanwhile, genes encoding Group A protein phosphatases, PP2Cs, kinases, and SnRK2s were up-regulated in the root and shoot under HN as well. In rice, differential expression of several PP2C/SnRK2 was reported under abiotic stress and ABA treatment (Xue et al., 2008), and they are known to serve as key regulators of ABA signaling in stresses such as desiccation (Komatsu et al., 2013). This shows that ABA plays a crucial role in rice under the early stages of NH_4^+ toxicity. In addition, *EIN3* and *ERF* genes (*AP2/EREBP*), regulating stress response and development programs (Kazan, 2015), were up-regulated under HN, but only in the root (Supplementary File S3). ET often acts cooperatively with JA and SA, and their biosynthesis, transport, and

accumulation trigger a cascade of signaling pathways involved in plant defense (Matilla-Vazquez and Matilla, 2014). We found transcripts of *MYC2*, involved in JA synthesis, and *PR1*, involved in SA synthesis, were also up-regulated mainly in the root (Table 1). Furthermore, Aux/IAA transcripts in the shoot were up-regulated (Supplementary File S1); auxin signaling is an integral part in plant adaptation to salinity stress (Fahad et al., 2015). Meanwhile, brassinosteroids (BR) signaling is regulated by BRI1, and the expression level of BRI1 was increased at the two time points and increased over time. However, BRI1 was only expressed in the shoot at 4 h, returning to a normal level at 12 h (Supplementary File S3). It has been shown that BRs are involved in plant growth and development in Arabidopsis via the key regulator BRI1 (Jaillais and Vert, 2016). These data uncovered the spatial specificity in hormone signaling under HN. This provides important clues about the engagement of the key phytohormones in rice in response to NH_4^+ stress.

5. Conclusions

NH_4^+ profoundly affects various aspects of plant cell development and metabolism. Plants differ greatly in their abilities to process the NH_4^+ ion and in their toxicity thresholds as soil NH_4^+ becomes elevated. Research into the responses to NH_4^+at the genome-wide level in rice, a model system for NH_4^+ tolerance, will allow for a greatly improved understanding of the physiological and molecular mechanisms underlying the NH_4^+ toxicity syndrome. The present study provides a first spatio-temporal specificity analysis of the rice genome in response to NH_4^+ toxicity. Our gene expression analysis results reveal key adjustments in the biosynthesis and regulation of phytohormones in rice in response to NH_4^+ and uncover the intricate metabolite regulation network at play in response to the ionic stress. Rice has the ability to redirect ions and nutrients to prioritized processes and induce adequate metabolic adjustments for survival when challenged with high NH_4^+. It is hoped that the molecular identification and characterization of the phenomenon of NH_4^+ tolerance will help direct the improvement of NH_4^+ tolerance in crop plants, many of which are highly susceptible to NH_4^+ toxicity at low to intermediate soil concentrations.

Acknowledgements

This work was supported by grant of the National Natural Science Foundation of China (31430095, 31501821 and 31300210), China Postdoctoral Science Foundation (2015T80593), and a Natural Sciences and Engineering Research Council of Canada (NSERC) grant to HJK (RGPIN-2014-05650).

Appendix A. Supplementary data

Supplementary data associated with this article can be found, in the online version, at http://dx.doi.org/10.1016/j.jplph.2017.02.006.

References

Abdi, H., 2007. The bonferroni and Sidak corrections for multiple comparisons. In: Salkind, N.J. (Ed.), Encyclopedia of Measurement and Statistics. Sage, Thousand Oaks, CA.

Bai, L., Ma, X., Zhang, G., Song, S., Zhou, Y., Gao, L., Miao, Y., Song, C.P., 2014. A receptor-like kinase mediates ammonium homeostasis and is important for the polar growth of root hairs in *Arabidopsis*. Plant Cell. 26, 1497–1511.

Balkos, K.D., Britto, D.T., Kronzucker, H.J., 2010. Optimization of ammonium acquisition and metabolism by potassium in rice (*Oryza sativa* L. cv. IR-72). Plant Cell Environ. 33, 23–34.

Bittsánszky, A., Pilinszky, K., Gyulai, G., Komives, T., 2015. Overcoming ammonium toxicity. Plant Sci. 231, 184–190.

Britto, D.T., Kronzucker, H.J., 2002. NH_4^+ toxicity in higher plants: a critical review. J. Plant Physiol. 159, 567–584.

Britto, D.T., Siddiqi, M.Y., Glass, A.D., Kronzucker, H.J., 2001. Futile transmembrane NH4(+) cycling: a cellular hypothesis to explain ammonium toxicity in plants. Proc. Natl. Acad. Sci. U. S. A. 98, 4255–4258.

Britto, D.T., Balkos, K.D., Becker, A., Coskun, D., Huynh, W.Q., Kronzucker, H.J., 2014. Potassium and nitrogen poising: physiological changes and biomass gains in rice and barley. Can. J. Plant Sci. 94, 1085–1089.

Buer, C.S., Muday, G.K., Djordjevic, M.A., 2007. Flavonoids are differentially taken up and transported long distances in *Arabidopsis*. Plant Physiol. 145, 478–490.

Chandran, A.K.N., Jung, K.H., 2014. Resources for systems biology in rice. J. Plant Biol. 57, 80–92.

Cock, P.J., Fields, C.J., Goto, N., Heuer, M.L., Rice, P.M., 2010. The Sanger FASTQ file format for sequences with quality scores, and the Solexa/Illumina FASTQ Variants. Nucleic Acids Res. 38, 1767–1771.

Conrath, U., Beckers, G.J., Langenbach, C.J., Jaskiewicz, M.R., 2015. Priming for enhanced defense. Annu. Rev. Phytopathol. 53, 97–119.

Conrath, U., 2011. Molecular aspects of defense priming. Trends Plant Sci. 16, 524–531.

Cutler, S.R., Rodriguez, P.L., Finkelstein, R.R., Abrams, S.R., 2010. Abscisic acid: emergence of a core signaling network. Annu. Rev. Plant Biol. 61, 651–679.

Domínguez-Valdivia, M.D., Aparicio-Tejo, P.M., Lamsfus, C., Cruz, C., Martins-Loução, M.A., Moran, J.F., 2008. Nitrogen nutrition and antioxidant metabolism in ammonium-tolerant and -sensitive plants. Plant Physiol. 132, 359–369.

Fahad, S., Hussain, S., Bano, A., Saud, S., Hassan, S., Shan, D., Khan, F.A., Khan, F., Chen, Y.T., Wu, C., Tabassum, M.A., Chun, M.X., Afzal, M., Jan, A., Jan, M.T., Huang, J.L., 2015. Potential role of phytohormones and plant growth-promoting rhizobacteria in abiotic stresses: consequences for changing environment. Environ. Sci. Pollut. Res. 22, 4907–4921.

Fan, X.R., Xie, D., Chen, J.G., Lu, H.Y., Xu, Y.L., Ma, C.H., Xu, G.H., 2014. Over-expression of *OsPTR6* in rice increased plant growth at different nitrogen supplies but decreased nitrogen use efficiency at high ammonium supply. Plant Sci. 227, 1–11.

Flowers, T.J., Colmer, T.D., 2015. Plant salt tolerance: adaptations in halophytes. Ann. Bot. 115, 327–331.

Guan, M., de Bang, T.C., Pedersen, C., Schjoerring, J.K., 2016. Cytosolic glutamine synthetase Gln1;2 is the main isozyme contributing to GS1 activity and can be up-regulated to relieve ammonium toxicity. Plant Physiol. 171, 1921–1933.

Hare, P.D., Cress, W.A., Staden, J.V., 1998. Dissecting the roles of osmolyte accumulation during stress. Plant Cell Environ. 21, 535–553.

Heil, M., Baldwin, I.T., 2002. Fitness costs of induced resistance: emerging experimental support for a slippery concept. Trends Plant Sci. 7, 61–67.

Jaillais, Y., Vert, G., 2016. Brassinosteroid signaling and BRI1 dynamics went underground. Curr. Opin. Plant Biol 33, 92–100.

Kazan, K., 2015. Diverse roles of jasmonates and ethylene in abiotic stress tolerance. Trends Plant Sci. 20, 219–229.

Komatsu, K., Suzuki, N., Kuwamura, M., Nishikawa, Y., Nakatani, M., Ohtawa, H., Takezawa, D., Seki, M., Tanaka, M., Taji, T., Hayashi, T., Sakata, Y., 2013. Group A PP2Cs evolved in land plants as key regulators of intrinsic desiccation tolerance. Nat. Commun. 4, 2219.

Kronzucker, H.J., Glass, A.D., Siddiqi, M.Y., 1999. Inhibition of nitrate uptake by ammonium in barley. Analysis Of component fluxes. Plant Physiol. 120, 283–292.

Kronzucker, H.J., Glass, A.D., Siddiqi, M.Y., Kirk, G.J.D., 2000. Comparative kinetic analysis of ammonium and nitrate acquisition by tropical lowland rice: implications for rice cultivation and yield potential. New Phytol. 145, 471–476.

Langmead, B., Trapnell, C., Pop, M., Salzberg, S.L., 2009. Ultrafast and memory-efficient alignment of short DNA sequences to the human genome. Genome Biol. 10, 25–34.

Li, H., Durbin, R., 2009. Fast and accurate short read alignment with Burrows-Wheeler transform. Bioinformatics 25, 1754–1760.

Li, B.H., Li, G.J., Kronzucker, H.J., Baluska, F., Shi, W.M., 2014. Ammonium stress in *Arabidopsis*: signaling, genetic loci, and physiological targets. Trends Plant Sci. 19, 107–114.

Lv, W.T., Lin, B., Zhang, M., Hua, X.J., 2011. Proline accumulation is inhibitory to *Arabidopsis* seedlings during heat stress. Plant Physiol. 156, 1921–1933.

Ma, X.L., Zhu, C.H., Yang, N., Gan, L.J., Xia, K., 2016. γ-Aminobutyric acid addition alleviates ammonium toxicity by limiting ammonium accumulation in rice (*Oryza sativa*) seedlings. Plant Physiol. 158, 389–401.

Matilla-Vazquez, M.A., Matilla, A.J., 2014. Ethylene:Role in plants under environmental stress. In: Ahmad, P., Wani, M.R. (Eds.), Physiological Mechanisms and Adaptation Strategies in Plants Under Changing Environment, 2. Springer Science+ Business Media, New York, pp. 63–94.

Mishra, N.S., Tuteja, R., Tuteja, N., 2006. Signaling through MAP kinase networks in plants. Arch. Biochem. Biophys. 452, 55–68.

Naoumkina, M.A., Zhao, Q., Gallego-Giraldo, L., Dai, X., Zhao, P.X., Dixon, R.A., 2010. Genome-wide analysis of phenylpropanoid defense pathways. Mol. Plant Pathol. 11, 829–846.

Nguyen, H.N., Kim, J.H., Hyun, W.Y., Nguyen, N.T., Hong, S.W., Lee, H., 2013. TTG1-mediated flavonols biosynthesis alleviates root growth inhibition in response to ABA. Plant Cell Rep. 32, 503–514.

Peer, W.A., Murphy, A.S., 2007. Flavonoids and auxin transport: modulators or regulators? Trends Plant Sci. 12, 556–563.

Peleg, Z., Blumwald, E., 2011. Hormone balance and abiotic stress tolerance in crop plants. Curr. Opin. Plant Biol. 14, 290–295.

Ranathunge, K., El-Kereamy, A., Gidda, S., Bi, Y.M., Rothstein, S.J., 2014. *AMT1;1* transgenic rice plants with enhanced NH_4^+ permeability show superior growth

and higher yield under optimal and suboptimal NH_4^+ conditions. J. Exp. Bot. 65, 965–979.
Ranathunge, K., Schreiber, L., Bi, Y.M., Rothstein, S.J., 2016. Ammonium-induced architectural and anatomical changes with altered suberin and lignin levels significantly change water and solute permeabilities of rice (*Oryza sativa* L.) roots. Planta 243, 231–249.
Saxena, S.C., Kaur, H., Verma, P., Petla, B.P., Andugula, V.R., Majee, M., 2013. Osmoprotectants: potential for crop improvement under adverse conditions. In: Tuteja, N., Singh, S.G. (Eds.), Plant Acclimation to Environmental Stress. Springer, NewYork, NY, pp. 197–232.
Shulaev, V., Cortes, D., Miller, G., Mittler, R., 2008. Metabolomics for plant stress response. Plant Physiol. 132, 199–208.
Sonoda, Y., Ikeda, A., Saiki, S., von Wirén, N., Yamaya, T., Yamaguchi, J., 2003. Distinct expression and function of three ammonium transporter genes (OsAMT1;1-1;3) in rice. Plant Cell Physiol. 44, 726–734.
Szczerba, M.W., Britto, D.T., Balkos, K.D., Kronzucker, H.J., 2008. Alleviation of rapid, futile ammonium cycling at the plasma membrane by potassium reveals K^+-sensitive and −insensitive components of NH_4^+ transport. J. Exp. Bot. 59, 303–313.
Vob, U., Bishopp, A., Farcot, E., Bennett, M.J., 2014. Modelling hormonal response and development. Trends Plant Sci. 19, 311–319.
Wang, W., Li, R., Zhu, Q., Tang, X., Zhao, Q., 2016. Transcriptomic and physiological analysis of common duckweed Lemna minor responses to NH_4^+ toxicity. BMC Plant Biol. 16, 92.
Xie, Y.J., Mao, Y., Xu, S., Zhou, H., Duan, X.L., Cui, W.T., Zhang, J., Xu, G.H., 2015. Heme-heme oxygenase 1 system is involved in ammonium tolerance by regulating antioxidant defense in Oryza sativa. Plant Cell Environ. 38, 129–143.
Xue, T., Wang, D., Zhang, S., Ehlting, J., Ni, F., Jakab, S., Zheng, C., Zhong, Y., 2008. Genome-wide and expression analysis of protein phosphatase 2C in rice and *Arabidopsis*. BMC Genomics 20, 550.
Yang, S.Y., Hao, D.L., Song, Z.Z., Yang, G.Z., Wang, L., Su, Y.H., 2015a. RNA-Seq analysis of differentially expressed genes in rice under varied nitrogen supplies. Gene 555, 305–317.
Yang, H.Y., von der Fecht-Bartenbach, J., Friml, J., Lohmann, J.U., Neuhauser, B., Ludewig, U., 2015b. Auxin-modulated root growth inhibition in *Arabidopsis thaliana* seedlings with ammonium as the sole nitrogen source. Funct. Plant Biol. 42, 239–251.
Zhang, Y., Fonslow, B.R., Shan, B., Baek, M.C., Yates III, J.R., 2013. Protein analysis by shotgun/bottom-up proteomics. Chem. Rev. 10, 234–294.
Zhao, Q., Zhang, H., Wang, T., Chen, S.X., Dai, S.J., 2013. Proteomics-based investigation of salt-responsive mechanisms in plant roots. J. Proteomics 82, 230–253.
Zheng, X., He, K., Kleist, T., Chen, F., Luan, S., 2015. Anion channel SLAH3 functions in nitrate-dependent alleviation of ammonium toxicity in *Arabidopsis*. Plant Cell Environ. 38, 474–486.